SPACECRAFT INSERTION INTO HIGH WORKING ORBITS USING LIGHT-CLASS LAUNCHER AND ELECTRIC PROPULSION

Vyacheslav PETUKHOV
Mikhail KONSTANTINOV

Moscow State Aviation Institute
Volokolamskoye shosse 4, Post box A-80, GSP-3, Moscow, 125993, Russia
petukhov@mtu-net.ru
konfed@cosmos.com.ru

ABSTRACT *– It is considered minimum-time transfer between elliptical and circular orbits. The optimization technique for multirevolutional low-thrust transfer is presented. It is presented the universal table of non-dimensional characteristic velocities, which could be used for fast estimation of optimal transfers between arbitrary elliptical and circular orbits. This technique is applied to the optimization of spacecraft insertion into target orbits using light-class launch vehicles and electric propulsion. Typical flight profile includes insertion into a parking orbit using launch vehicle, transfer into an elliptical intermediate orbit using high-thrust, and transfer into target orbit using electric propulsion. Presented results could be used for feasibility study of low-cost space missions.*

KEYWORDS: low-thrust trajectory, optimization, minimum-time transfer, universal table.

INTRODUCTION

Electric propulsion is becoming a routine tool for spacecraft (SC) station-keeping and insertion into the target orbits. Nevertheless, low-thrust mission analysis remains a hard problem as a routine too. It is connected with necessity to solve difficult boundary value or optimal control problems [1-4]. As a rule, such kind of problems could be solved numerically only and their solving is become complicated by numerical sensitivity, instability, and solutions branching. This paper presents versatile tool for optimization and feasibility study of low-thrust missions connected with transfers from an elliptical orbit into the circular target orbit. This tool is universal table of characteristic velocity for minimum-time transfers, allowing calculate low-thrust transfer parameters by simple interpolation. This table was filled using low-thrust trajectory optimization technique described in [5-7].

One of low-thrust advantages is reducing of requirements to the launch vehicles (LV). For example, light-class LV could be used for insertion SC into high target orbit [8, 9], in particularity, into geostationary orbit (GEO). Unfortunately, low thrust acceleration level leads to the very long-duration transfers. Trade-off between transfer duration and payload maximization is realized by combined flight profile. In this case, high-thrust (chemical) propulsion system inserts SC into an intermediate orbit and SC electric propulsion provides transfer from the intermediate orbit into the target orbit.

The study was partially supported by grants of Russian Foundation for Fundamental Research 03-01-00864 and 01-01-00015

We consider transfers using light-class LV (1500-4000 kg in the parking orbit), jettisonable bi-propellant propulsion unit (BPPU), and SC electric propulsion. Scaling and interpolation over the universal table was used for optimal low-thrust trajectory estimation. Presented application demonstrates usefulness, ease, and versatility of this technique for feasibility study. In particularity, this technique provides easy estimation of SC mass versus design parameters variations, such as transfer duration, high- and low-thrust propulsion systems parameters, etc.

The problem is to deliver SC having maximum final mass into the target orbit for a given transfer duration. It is considered following flight profile. LV inserts into parking orbit payload which consists of SC, BPPU, and adapter. BPPU provides insertion into an intermediate orbit and then separates from SC. SC is delivered from the intermediate orbit into the target orbit using electric propulsion system (EPS).

There are used following nominal values of design parameters. Adapter mass is 50 kg. BPPU main engine has thrust 400 N and specific impulse 308 s. BPPU final mass is following [10]:

$$m_f^{BPPU} = m_{f0}^{BPPU} + a_t m_p ,$$

where $m_{f0}^{BPPU} = 140$ kg, $a_t = 0.1$, m_p – active propellant mass. EPS has specific impulse $I_{sp}^{EPT} = 1500$ s. Electric propulsion thruster efficiency is following:

$$\eta_{EPT} = \frac{a}{1 + \left(\frac{b}{I_{sp}^{EPT} g_0} \right)^2} ,$$

where $a = 0.661$, $b = 10000$, $g_0 = 9.80665$ m/s^2. EPS thrust is

$$P = \frac{2\eta_{PPU}\eta_{PPT} N_e}{I_{sp}^{EPT} g_0} ,$$

where $\eta_{PPU} = 0.9$ – power processing unit efficiency, $N_e = 3000$ W – EPS electrical power.

There are considered launches from Plesetsk and Kourou launch sites. The parking orbit radius is 6571 km in both cases, and initial inclination is 63° for Plesetsk and 7° for Kourou. The target orbit radius is 42171 km and inclination 0° (GEO) or radius 25471 km and inclination 64.8° (Glonass orbit). Rockot, Angara-1.1, and Angara-1.2 LV are considered. These LV delivers payload 1950, 2000, and 3700 kg into the parking orbit from Plesetsk [11]. In addition, it is considered an advanced Rockot LV using modified 3rd stage. Its payload is assumed equals to 2700 kg in the circular parking orbit having altitude 200 km and inclination 63°.

PROBLEM DECOMPOSITION

The combined flight profile consists of two phases. During high-thrust phase SC is delivered from given parking orbit into an intermediate orbit. Goal of low-thrust phase is SC insertion from this intermediate orbit into the target orbit. We consider circular target orbit, but intermediate orbit can be arbitrary. Taking into account symmetry reasons, it can be proved that apsidal line of intermediate orbit should belong to the plane of target orbit. Let reference plane coincides with the target orbit plane (i.e. target orbit inclination equals to 0). In this case only 3 parameters of intermediate orbit have significance, namely there are apogee/perigee altitudes and inclination.

So, the trajectory optimization problem divides into two sub-problems: 1) optimization of high-thrust transfer from the parking orbit into an intermediate orbit, and 2) optimization of low-thrust transfer from the intermediate orbit into the target orbit. This decomposed problem has 3 free parameters (perigee/apogee altitudes and inclination of intermediate orbit), which should be optimized also.

While the first sub-problem is trivial, the optimization of low-thrust phase remains quite difficult. But due to novel numerical techniques and new developed software [5-7] it becomes feasible to carry out optimization of numerous low-thrust trajectories on the relatively dense grid of intermediate orbit

parameters. As result the table of required characteristic velocity on this grid was filled. Low-thrust trajectories were optimized using Pontryagin's maximum principle and averaging technique. Due to averaging, the computed optimal trajectories are asymptotic. Therefore these results are correct for any SC parameters while averaging assumptions are held true. Moreover, these trajectories could be scaled for a given target orbit altitude, and primary gravitational parameter. Of course, grid of intermediate orbit parameters should be scaled too in this case. For minimum-time transfer to GEO the grid nodes are 200, 1000, 5000, 10000, 20000, 35800, 45000, 60000, 80000, 100000, 120000, 140000, 160000, and 180000 km for intermediate orbit perigee and apogee altitudes and 0, 15, 30, 45, 60, 75, and 90 degrees for intermediate orbit inclination. Required characteristic velocity in the intermediate points was computed using 3D linear interpolation over the grid.

So, considered optimization problem reduces to final SC mass maximization with respect to apogee/perigee altitudes, and inclination of intermediate orbit while high-thrust phase is optimized using well-known infinite-thrust technique, and parameters of optimal low-thrust phase are interpolated from pre-computed grid.

METHODOLOGY OF LOW-THRUST TRAJECTORY OPTIMIZATION

Equations of Motion

It is considered spacecraft motion under the influence of the primary gravity force and electric propulsion thrust. Magnitudes of the thrust and specific impulse of running electric propulsion engine are assumed to be constant. There are not applied any constraints to the thrust direction. Gravity force is obeyed to the inverse square law. Effects of eclipses and solar array degradation are ignored. There are analyzed transfers without thrust switching.

Thrust acceleration projections into orbital orts are following:

$$a_\tau = \frac{P}{m}\cos\vartheta\cos\psi\ ,\ a_r = \frac{P}{m}\sin\vartheta\cos\psi\ ,\ a_n = \frac{P}{m}\sin\psi\ , \tag{1}$$

where a_τ, a_r, a_n – circumferential, radial, and binormal projection of thrust acceleration correspondingly, P – thrust magnitude, m – spacecraft mass, ϑ - «pitch» angle (angle between projection of thrust vector onto the orbital plane and circumferential vector), ψ - «yaw» angle (angle between thrust vector and orbital plane).

To avoid singularity for small eccentricity and inclination, there are used equations of motion in the equinoctial elements [12]:

$$\left.\begin{aligned}
\frac{dh}{dt} &= \frac{P}{m}\frac{h}{\xi}\cdot h\cos\vartheta\cos\psi,\\
\frac{de_x}{dt} &= \frac{P}{m}\frac{h}{\xi}\left\{\xi\sin F\sin\vartheta\cos\psi + \left[(\xi+1)\cos F + e_x\right]\cos\vartheta\cos\psi - e_y\eta\sin\psi\right\},\\
\frac{de_y}{dt} &= \frac{P}{m}\frac{h}{\xi}\left\{-\xi\cos F\sin\vartheta\cos\psi + \left[(\xi+1)\sin F + e_y\right]\cos\vartheta\cos\psi + e_x\eta\sin\psi\right\},\\
\frac{di_x}{dt} &= \frac{P}{m}\frac{h}{\xi}\cdot\frac{1}{2}\varphi\cos F\sin\psi,\\
\frac{di_y}{dt} &= \frac{P}{m}\frac{h}{\xi}\cdot\frac{1}{2}\varphi\sin F\sin\psi,\\
\frac{dF}{dt} &= \frac{\xi^2}{h^3} + \frac{P}{m}\frac{h}{\xi}\cdot\xi\eta\sin\psi,\\
\frac{dm}{dt} &= -\frac{P}{w},
\end{aligned}\right\} \tag{2}$$

where $h=\sqrt{\frac{p}{\mu}}$, $e_x=e\cos(\Omega+\omega)$, $e_y=e\sin(\Omega+\omega)$, $i_x=\tan\frac{i}{2}\cos\Omega$, $i_y=\tan\frac{i}{2}\sin\Omega$, and $F=\nu+\omega+\Omega$ - equinoctial elements, p – semi-latus rectum, e – eccentricity, ω - argument of pericenter, i – inclination, Ω - right ascension of ascending node, ν - true anomaly, $\xi=1+e_x\cos F+e_y\sin F$, $\eta=i_x\sin F-i_y\cos F$, $\varphi=1+i_x^2+i_y^2$, w – exhaust velocity of electric propulsion.

It is necessary to transfer spacecraft having initial mass m_0 from the initial orbit

$$h=h_0,\ e_x=e_{x0},\ e_y=e_{y0},\ i_x=i_{x0},\ i_y=i_{y0} \tag{3}$$

into the final one

$$h=h_k,\ e_x=e_{xk},\ e_y=e_{yk},\ i_x=i_{xk},\ i_y=i_{yk} \tag{4}$$

for a time T.

It is considered the minimization of performance index

$$J=\int_0^T dt\to\min, \tag{5}$$

which corresponds to the minimum-time problem.

Optimal Control

The maximum principle is used to solve the problem (2-5). The Hamiltonian of optimal control problem (2-5) is

$$H=-1+\frac{\xi^2}{h^3}p_F+\frac{P}{m}\frac{h}{\xi}\left(A_\tau\cos\vartheta\cos\psi+A_r\sin\vartheta\cos\psi+A_n\sin\psi\right) \tag{6}$$

where

$$A_\tau=hp_h+\left[(\xi+1)\cos F+e_x\right]p_{ex}+\left[(\xi+1)\sin F+e_y\right]p_{ey},$$

$$A_r=\xi\left(\sin F\cdot p_{ex}-\cos F\cdot p_{ey}\right),$$

$$A_n=\eta\left(-e_y p_{ex}+e_x p_{ey}\right)+\frac{1}{2}\varphi\left(\cos F\cdot p_{ix}+\sin F\cdot p_{iy}\right)+\xi\eta\cdot p_F,$$

p_h, p_{ex}, p_{ey}, p_{ix}, p_{iy}, p_F –adjoint variables, coupled with the phase coordinates h, e_x, e_y, i_x, i_y, and F correspondingly.

Optimal controls $\vartheta(t)$, $\psi(t)$ are defined from the Hamiltonian (6) maximization:

$$\cos\vartheta=\frac{A_\tau}{\sqrt{A_\tau^2+A_r^2}},\ \sin\vartheta=\frac{A_r}{\sqrt{A_\tau^2+A_r^2}}, \tag{7}$$

$$\cos\psi=\frac{\sqrt{A_\tau^2+A_r^2}}{\sqrt{A_\tau^2+A_r^2+A_n^2}},\ \sin\psi=\frac{A_n}{\sqrt{A_\tau^2+A_r^2+A_n^2}}, \tag{8}$$

Within the minimum-time problem, differential equation for m can be eliminated using explicit expression for the spacecraft mass:

$$m=m_0-(P/w)\cdot t. \tag{9}$$

Substitution of (7) and (8) into (6) leads to the expression for the optimal Hamiltonian:

$$H=-1+\frac{P}{m}\frac{h}{\xi}\left(A_\tau^2+A_r^2+A_n^2\right)^{1/2}+\frac{\xi^2}{h^3}p_F=-1+kPA+H_F, \tag{10}$$

where $k=\frac{1}{m}\frac{h}{\xi}$, $A=\left(A_\tau^2+A_r^2+A_n^2\right)^{1/2}$, $H_F=\frac{\xi^2}{h^3}p_F$.

Since the transfer between orbits is considered, the final true longitude F is not fixed, therefore $p_F(T)=0$. The optimal Hamiltonian does not depend on F after averaging, therefore

$\frac{dp_F}{dt} = -\frac{\partial H}{\partial F} = 0$. So, $p_F \equiv 0$ on the averaged solution. The optimal Hamiltonian, taking into account supposed averaging, becomes following:

$$H = -1 + kPA, \tag{11}$$

and the equations of motion become following:

$$\left.\begin{aligned} \frac{d\mathbf{x}}{dt} &= \frac{\partial H}{\partial \mathbf{p}} = P\left[k\left(A_\tau \frac{\partial A_\tau}{\partial \mathbf{p}} + A_r \frac{\partial A_r}{\partial \mathbf{p}} + A_n \frac{\partial A_n}{\partial \mathbf{p}}\right)A^{-1}\right], \\ \frac{d\mathbf{p}}{dt} &= -\frac{\partial H}{\partial \mathbf{x}} = -P\left[\frac{\partial k}{\partial \mathbf{x}} A + k\left(A_\tau \frac{\partial A_\tau}{\partial \mathbf{x}} + A_r \frac{\partial A_r}{\partial \mathbf{x}} + A_n \frac{\partial A_n}{\partial \mathbf{x}}\right)A^{-1}\right] \end{aligned}\right\} \tag{12}$$

Averaging

Low thrust-to-gravity acceleration ratio allows to use averaging of optimal differential equations. The averaging allows to increase the integration step size and, therefore, to decrease computational consumptions. But main reason of averaging usage is its regularizing role: the averaged differential equations are more stable numerically in comparison with non-averaged ones.

The averaging on time over the spacecraft orbital period is used. The averaging asymptotic basis is well-known: solution of averaged differential equations is zero-order term of the Fourier series expansion of non-averaged solution. The intuitive basis of the averaging is confined in the smallness variation of the slow orbital elements during one revolution due to low thrust.

Differential equations are averaged using following expression:

$$\frac{d\mathbf{y}}{dt} = \frac{1}{T}\int_{t_0}^{t_0+T} \mathbf{r}(\mathbf{y}, F, t)dt = \frac{n}{2\pi}\int_0^{2\pi} \mathbf{r}(\mathbf{y}, F, t)\frac{dt}{dF}dF, \tag{13}$$

where $\mathbf{y}=(\mathbf{x}^T, \mathbf{p}^T)^T$, $\mathbf{r}(\mathbf{y},F,t)$ – the right parts of non-averaged differential equations (12), $n = \frac{1}{\mu}\left[\sqrt{1-e_x^2-e_y^2}/h\right]^3$ - mean motion, $dt/dF = h^3/\xi^2$.

Boundary Value Problem

State vector $\mathbf{x}$, co-state vector $\mathbf{p}$, and residual vector $\mathbf{f}$ at the final time T are computed as result of integration of equations (12) using averaging (13). Residual vector is following:

$$\mathbf{f} = \begin{pmatrix} h(T) - h_k \\ e_x(T) - e_{xk} \\ e_y(T) - e_{yk} \\ i_x(T) - i_{xk} \\ i_y(T) - i_{yk} \\ H(T) \end{pmatrix} = 0 \tag{14}$$

It is necessary to solve equations (14) with respect to vector of unknown TPBVP parameters $\mathbf{z}$. Vector $\mathbf{z}$ has form:

$$\mathbf{z} = \begin{pmatrix} \mathbf{p} \\ T \end{pmatrix} \tag{15}$$

for minimum-time problem.

Technique of the Boundary Value Problem Solving

The boundary value problem solving is reduced to the solving of nonlinear system, which is consisted of state residuals and transversality conditions. The continuation technique was used to solve this system. The continuation method belongs to the class of homotopic methods. One of the most simple version of continuation method was used in this study. The original problem is immersed into some

one-parametric family and then it is used the linear continuation of the problem solution with respect to the family parameter.
The essence of considered continuation technique is following. Let it is necessary to solve the nonlinear system

$$\mathbf{f}(\mathbf{z})=0. \tag{16}$$

Let $\mathbf{f}(\mathbf{z}_0)=\mathbf{b}$ at some initial approximation $\mathbf{z}_0$. Let us consider following one-parametric nonlinear system

$$\mathbf{f}_1(\mathbf{z},\tau)=\mathbf{f}(\mathbf{z})-(1-\tau)\mathbf{b}=0. \tag{17}$$

When $\tau=0$, $\mathbf{z}=\mathbf{z}_0$

$$\mathbf{f}_1(\mathbf{z}_0,\tau)=0, \tag{18}$$

and when $\tau=1$ $\mathbf{f}_1(\mathbf{z},\tau)=\mathbf{f}(\mathbf{z})$. Let us represent the solution of problem (17) as function of continuation parameter τ: $\mathbf{z}=\mathbf{z}(\tau)$. By virtue of (17), (18), $\mathbf{z}(\tau)$ can be represented as solution of the following system of ordinary differential equations:

$$\frac{d\mathbf{z}}{d\tau}=-\left[\frac{\partial\mathbf{f}(\mathbf{z})}{\partial\mathbf{z}}\right]^{-1}\mathbf{b} \tag{19}$$

having following initial condition:

$$\mathbf{z}(0)=\mathbf{z}_0. \tag{20}$$

After integrating the system (19), (20) on τ from 0 to 1, we get solution of the original problem (16). Thus, the solving of nonlinear system (16) is reduced formally to the initial value problem (19), (20). The system (19) we will name the differential equations system of continuation method.
If Euler method is used for problem (19), (20) integration, then the continuation method converts to the classical newton method. The advantage of continuation method in comparison with newton method appears if more advanced numerical integrators are used. If an ideal integration method is used, then the convergence domain of the continuation method in the parametric space $\mathbf{z}$ is coincided with the attraction area of given solution in this space. Equations (19) have singularity on the hypersurface where matrix $\partial\mathbf{f}/\partial\mathbf{z}$ is singular, therefore continuation method (as newton methods) is failed during crossing these hypersurfaces. Singularity of $\partial\mathbf{f}/\partial\mathbf{z}$ generally take place on the bounds of the attraction region of solution. The singularity is connected with a solution bifurcation of the original system (16).
Right parts of equations (12) are numerically averaged using expression (13) during integration corresponding system. The simple numerical techniques were used to get the integrals of functions. There are method of trapezoids or Simpson's method on the fixed uniform grid on F consisting of 30-300 nodes. The explicit Runge-Kutta method of 7th (8th) [13] order was used to integrate the averaging system (12). The initial conditions of basic problem were following:

$$\left.\begin{aligned} &h=h_0, e_x=e_{x0}, e_y=e_{y0}, i_x=i_{x0}, i_y=i_{y0},\\ &p_h=p_{h0}, p_{ex}=p_{ex0}, p_{ey}=p_{ey0}, p_{ix}=p_{ix0}, p_{iy}=p_{iy0}\end{aligned}\right\} \tag{21}$$

at the $t = 0$.
The continuation technique demonstrated its highly effectiveness for solving minimum-time problems. In most problems, the convergence to the optimal solution was achieved by choice the following initial approximation for TPBVP parameters vector:

$$p_h = 1, p_{ex} = p_{ey} = p_{ix} = p_{iy} = 0, T = 1,$$

where T – dimensionless time referred to the initial orbit. When parameters of the initial or final orbit were varied, the TPBVP parameters vector of previous problem was used as initial approximation.

UNIVERSAL TABLE FOR MINIMUM-TIME LOW-THRUST TRANSFERS BETWEEN ELLIPTICAL AND CIRCULAR ORBITS

Let consider dimensionless version of equations (13). Let gravitational parameter equals to 1, length unit equals to the target orbit radius r_k, and velocity unit is $\sqrt{\mu/r_k}$ Right parts of averaged differential equations (13) have multiplier P/m. Therefore these equations can be rewritten using characteristic velocity V_{ch} instead of t. So, minimum-time transfer from fixed initial orbit to the unit circular target orbit requires fixed non-dimensional characteristic velocity. Hence (optimal) transfer from orbit $\{r_\pi, r_\alpha, i\}$ to the circular equatorial orbit $\{r_k, r_k, 0\}$ requiring characteristic velocity V_{ch} is mapped to the

(optimal) transfer from orbit $\{qr_\pi, qr_\alpha, i\}$ to the circular equatorial orbit $\{qr_k, qr_k, 0\}$ requiring characteristic velocity $V_{ch}/\sqrt{q}$ (or $V_{ch}\sqrt{\mu_1/q\mu}$ if there are considered motions around different primaries having gravitational parameters μ and μ_1). Here r_π - pericenter radius, r_α - apocenter radius, i – inclination, q – arbitrary positive scalar; the apsidal line of initial orbit lies in the target orbit plane. Because it is considered motion in the inverse square gravity field, both initial and final orbits could be rotated on the same angle. So initial inclination i in the table should be interpreted as difference between final and initial inclinations.

This asymptotic property of (13) was used to construct versatile tool for low-thrust mission analysis. Namely, it was computed the table of non-dimensional characteristic velocity for 3D minimum-time transfers from elliptical orbits into unit circular orbit. There were computed 840 optimal trajectories corresponding to nodes of rectangular grid over initial r_π, r_α, and i. Above described scaling procedure and interpolation over the grid allow to obtain approximation of required characteristic velocity for minimum-time transfer from any elliptical orbit (within scaled grid) into any given circular target orbit. This table is presented in the Appendix.

INSERTION INTO GEO

Let consider SC insertion into the GEO using light-class LV. Fig. 1 presents final SC mass in GEO versus initial mass in the parking orbit and transfer duration. For example, Rockot or Angara-1.1 LV (payload 1950-2000 kg) provides insertion of SC having final mass 400 kg (500 kg) for 3 months (6 months), Angara-1.2 LV (payload 3700 kg) inserts 700 kg SC for 4 months. So, small telecommunication SC could be delivered into GEO using light-class LV from Plesetsk launch site for a reasonable transfer duration.

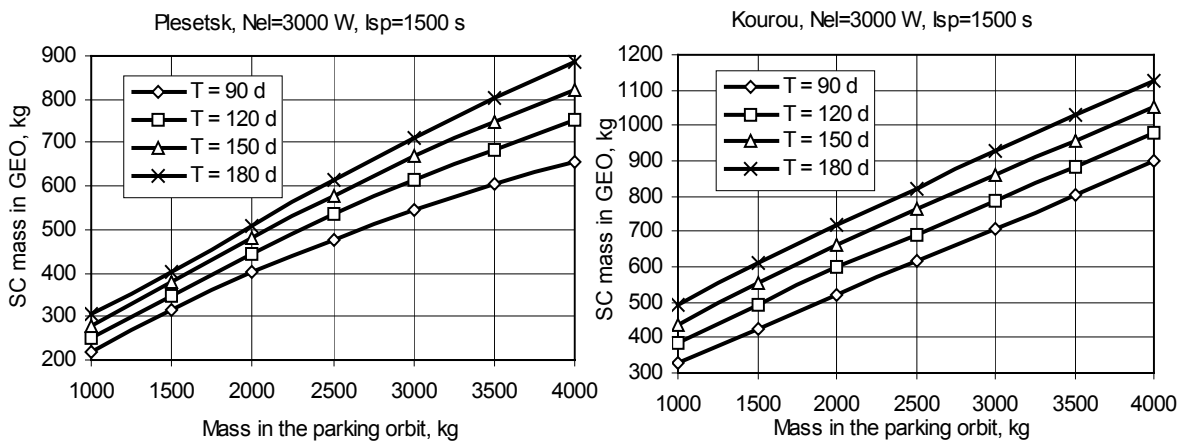

Fig. 1. Final SC mass in the GEO versus initial mass in the parking orbit and transfer duration, initial inclination 63° (left) and 7° (right)

Of course, near-equatorial launch site provides better mission performance. Left plot on Fig. 1 presents dependency of SC mass in GEO with respect to initial mass in the parking orbit and transfer duration for Kourou launch site. For example, final SC mass increases to 500 kg (700 kg) for transfer duration 3 months (6 months) if LV payload is 2000 kg. Plesetsk-based mission performance could be enhanced using more powerful EPS. Corresponding dependency of final SC mass with respect to LV payload and transfer duration for twice increased EPS electrical power (6 kW) is presented in the Fig. 2.

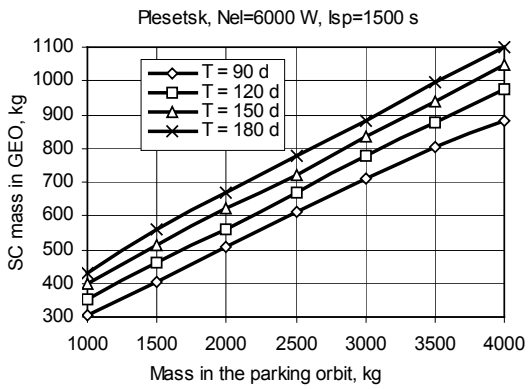

Fig. 2. Final SC mass in the GEO vs. initial mass and transfer duration (initial inclination 63°, EPS electrical power 6 kW)

Let consider Rockot LV. Dependency of SC final

mass versus EPS electrical power is presented in the Fig. 3. The EPS power increasing on 1500 W leads to 60-90 kg of SC mass in GEO.

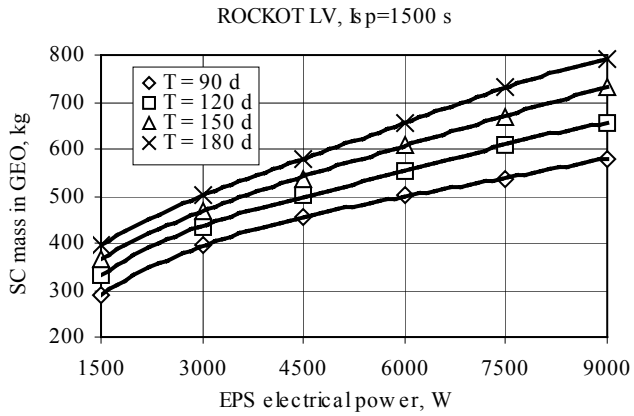

Fig. 3. Final SC mass as function of EPS electrical power

Fig. 4 shows impact of EPS specific impulse in final SC mass. It is seen that exists an optimal specific impulse for each given transfer duration. Its value increases from ~1540 s to ~1880 s when transfer duration increases from 90 days to 180 days. The maximums of final SC mass is flat enough: EPS specific impulse variation ±100 s relatively optimal value leads to final mass decreasing on 0.5-3 kg.

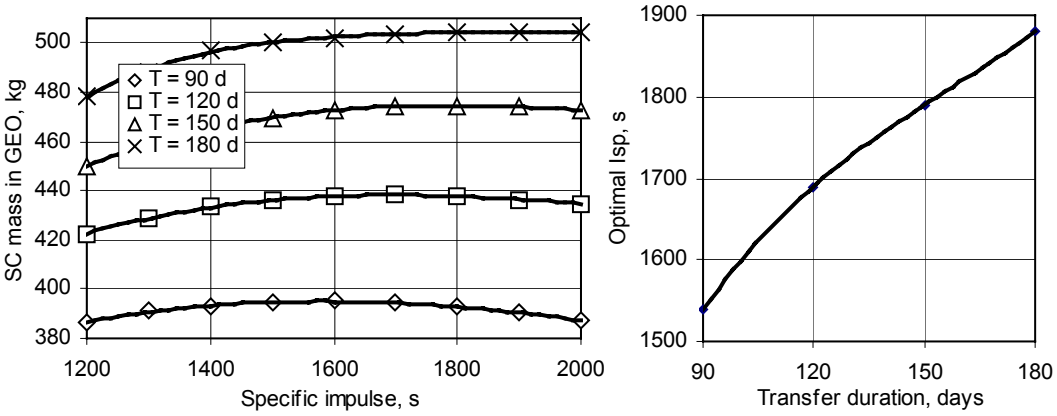

Fig. 4. EPS specific impulse optimization

Fig. 5 presents final SC mass as function of BPPU design parameters.

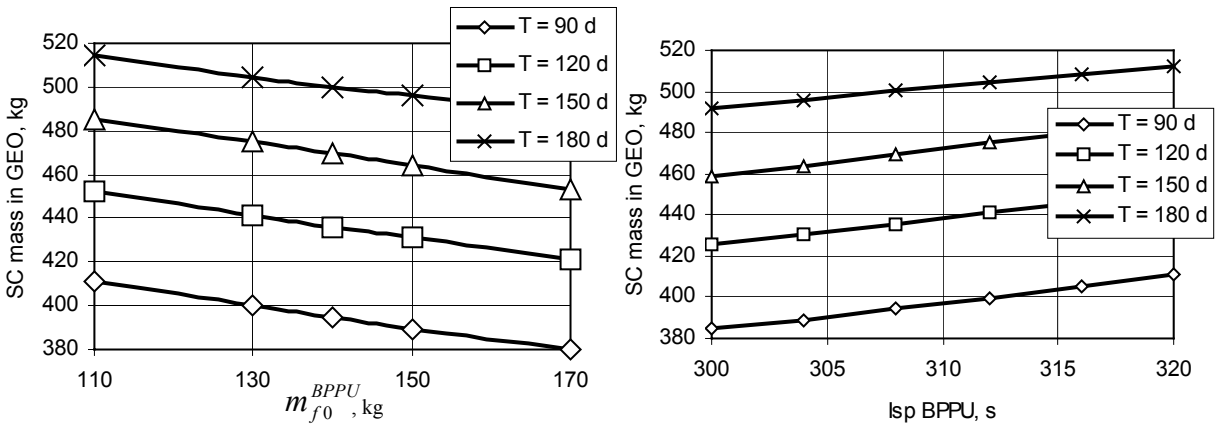

Fig. 5. Impact of BPPU parameters on final SC mass

It is seen that increasing of BPPU final mass on 10 kg leads to the ~5.5 kg decreasing of final SC mass. Increasing of BPPU specific impulse on 1 s leads to the increasing of final SC mass on 1.0-1.3 kg.

Fig. 6 presents optimal parameters of intermediate orbit as a function of transfer duration (EPS electrical power 1500 W). It is seen that the shorter transfer, the closely intermediate orbit to the target orbit. While transfer duration less than 150 days, apogee altitude remains approximately fixed (~100000 km) and intermediate orbit inclinations increases from 25° to 61°. Then this inclination remains fixed and apogee altitude decreases. Perigee altitude differs from minimum permissible value (here 500 km) for very short transfer only. Of course, perigee altitude increases when transfer duration decreases.

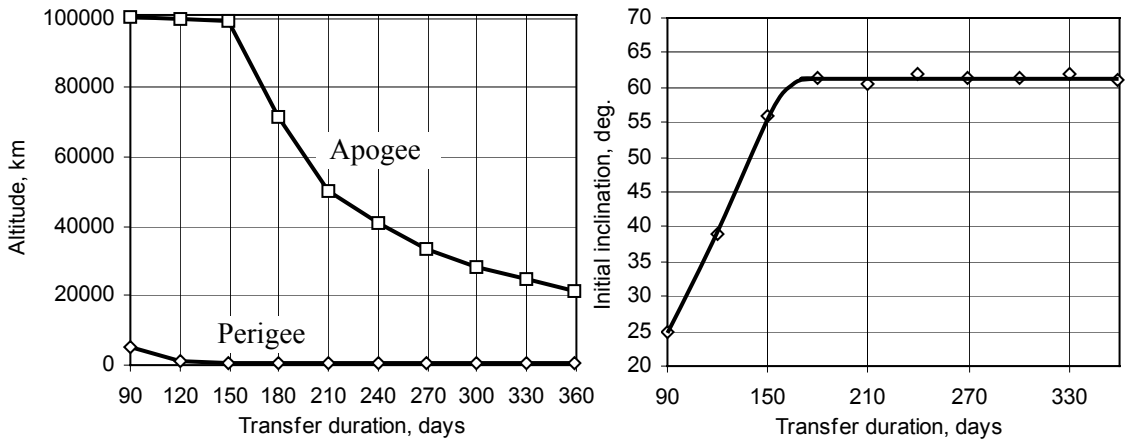

Fig. 6. Optimal intermediate orbit parameters vs. transfer duration (Rockot LV, EPS electrical power 1.5 kW, I_{sp} = 1500 s)

Fig. 7 presents main results of mission analysis for heavier LV: advanced Rockot and Angara-1.2.

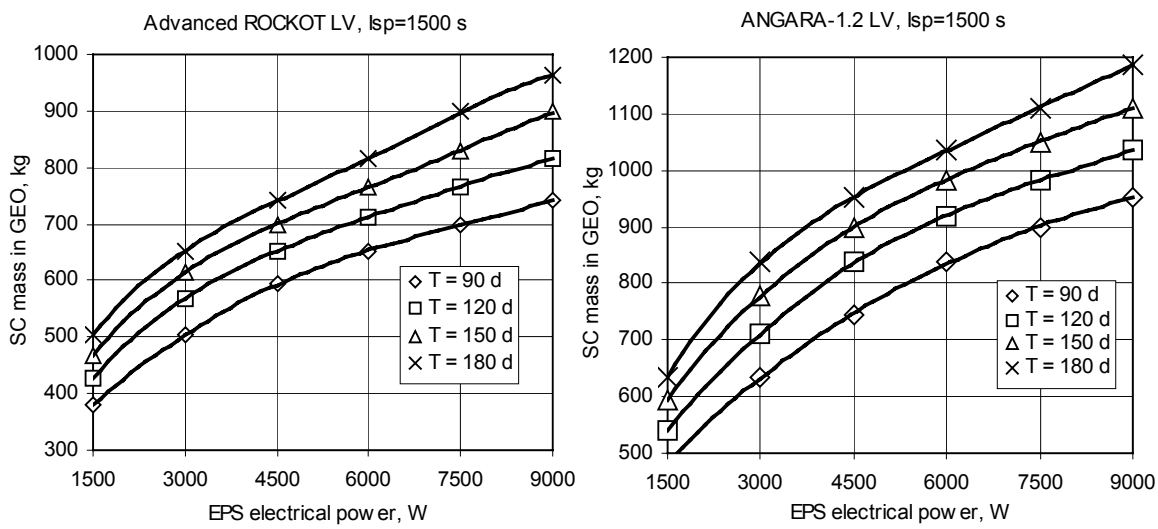

Fig. 7. Final SC mass vs. EPS electrical power for advanced Rockot and Angara-1.2 LV

INSERTION INTO GLONASS ORBIT

Let us consider insertion into GLONASS orbit using light-class LV and combined flight profile. Considered circular target orbit has altitude 19100 km and inclination 64.8°. Let LV inserts payload into the parking orbit having altitude 200 km and inclination 63°. So, required inclination increment is 1.8°. Fig. 8 summarizes results obtained for initial mass in the parking orbit within range 1500-4000 kg, EPS electrical power within range 3-6 kW, and transfer duration 120 days.

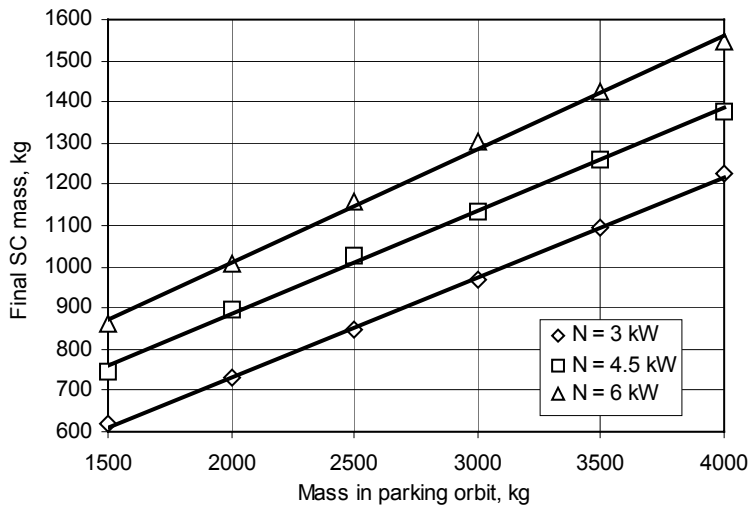

Fig. 8. Insertion into GLONASS orbit from Plesetsk launch site vs. LV payload and EPS electrical power (transfer duration 120 days)

CONCLUSION

New developed numerical methods and software allow solve the minimum-time problem in very wide range of initial conditions. Software robustness is assisted to compute table of the minimal required characteristic velocities for transfer into the circular orbit from an elliptical orbits, which orbital parameters are defined in nodes of relatively dense 3D-grid. Due to asymptotic property of obtained solutions, these results could be scaled to transfer into arbitrary circular target orbit. Such a way it was constructed the universal table of non-dimensional characteristic velocities. This table was used for low-thrust mission analysis.

It is presented the analysis of light-class LV using for SC insertion into high circular orbits. This analysis shows possibility to use such kind of LV for insertion geostationary communication satellites and navigational SC into target orbits from Plesetsk launch site. From the methodical point of view, this analysis demonstrates ease and versatility of proposed technique.

REFERENCES

[1] G.L. Grodzovsky, Yu.N. Ivanov, V.V. Tokarev. “Space Flight Mechanics. Optimization problems”. Moscow, Nauka, 1975, 703 pp. (in Russian)

[2] V.N. Lebedev. “Computation of Low-Thrust Spacecraft Motion”. Moscow, Comput. Center of USSR Academy of Sciences, 1968, 108 pp. (in Russian)

[3] M.S. Konstantinov. “Mathematical Programming Techniques for Flying Vehicles Design”. Moscow, Mashinostroeniye, 1975, 164 pp. (in Russian)

[4] Yu.A. Zakharov. Interorbital Spacecrafts Design. Moscow, Mashinostroeniye, 1984, 174 pp. (in Russian)

[5] V.G. Petukhov. “Low-Thrust Trajectory Optimization”. *Presentation at the Seminar on Space Flight Mechanics, Control, and Informatics*. Space Research Institute of Russian Academy of Science, June 2000 (http://arc.iki.rssi.ru/seminar/200006/OLTTE2.ppt)

[6] V. Petukhov. “Optimal Multirevolutional Transfers between Non-Coplanar Elliptical Orbits”. *Proceedings of International Symposium on Low Thrust Trajectories (LOTUS-2)*, Toulouse, France, 2002

[7] V. Petukhov. “Low-Thrust Trajectory Optimization in Russia”. *Presentation at the ESA/ESTEC Workshop on Trajectory Design and Optimisation*, Noordwijk, The Netherlands, 2002 (http://www.esa.int/gsp/ACT/Presentations/Petukhov/petukhov.ppt)

[8] A. Medvedev, V. Khatulev, V. Yuriev, V. Petukhov, M. Konstantinov. "Combined flight profile to insert telecommunication satellite into geostationary orbit using "Rockot" light-weight class launch vehicle". *51st International Astronautical Congress*. IAF-00-V.2.09, Rio de Janeiro, Brasilia, October 2-6, 2000

[9] A. Medvedev, V. Khatulev, V. Yuriev, V. Petukhov, A. Zakharov. "Lunar and Planetary Missions Using Rockot Launch Vehicle". IAA-L-0704P

[10] S.R. Oleson. "Mission Advantages of Constant Power, Variable Isp Electrostatic Thrusters". 36th AIAA/ASME/SAE/ASEE Joint Propulsion Conference and Exhibit, Huntsville, Alabama, July 16-19, 2000

[11] Http://www.khrunichev.com

[12] R.A. Broucke, P.J. Cefola. "On the Equinoctial Orbital Elements", *Celestial Mechanics*, Vol. 5, pp. 303-310, 1972

[13] F. Hairer, S.P. Norsett, G. Wanner. "Solving Ordinary Differential Equations I. Non-Stiff Problems". Spinger-Verlag, Berlin, 1987

APPENDIX

Table 1. Non-dimensional characteristic velocity for 3D minimum-time transfers from elliptical orbits into unit equatorial circular orbit.

Pericenter radius	$i = 0°$	$i = 15°$	$i = 30°$	$i = 45°$	$i = 60°$	$i = 75°$	$i = 90°$
	Apocenter radius = 0.15582						
0.15582	1.53333	1.64379	1.94186	2.33930	2.68257	2.99604	3.27018
	Apocenter radius = 0.17479						
0.15582	1.46214	1.57330	1.87295	2.25965	2.57992	2.87177	3.12976
0.17479	1.39190	1.50648	1.81226	2.21254	2.54324	2.83194	3.08299
	Apocenter radius = 0.26964						
0.15582	1.22458	1.31869	1.59000	1.90446	2.16797	2.39681	2.60069
0.17479	1.16029	1.26436	1.55469	1.88727	2.15571	2.38464	2.58598
0.26964	0.92579	1.06201	1.40264	1.80825	2.09596	2.31882	2.50702
	Apocenter radius = 0.38821						
0.15582	1.04558	1.12601	1.35157	1.60935	1.83278	2.02326	2.18983
0.17479	0.99428	1.08149	1.32781	1.60149	1.83122	2.02384	2.19064
0.26964	0.78136	0.90896	1.23845	1.57637	1.82259	2.01710	2.18041
0.38821	0.60495	0.77247	1.14757	1.54910	1.80517	1.99402	2.15027
	Apocenter radius = 0.62533						
0.15582	0.84640	0.91293	1.08062	1.27582	1.45390	1.60654	1.73681
0.17479	0.80606	0.87976	1.06435	1.27294	1.45821	1.61452	1.74686
0.26964	0.63868	0.74698	1.01121	1.27269	1.48031	1.64585	1.78236
0.38821	0.48000	0.63341	0.97679	1.28360	1.50168	1.66862	1.80434
0.62533	0.26457	0.51396	0.91989	1.29942	1.52180	1.68230	1.81254
	Apocenter radius = 0.86246						
0.15582	0.74740	0.80227	0.93753	1.09789	1.24928	1.38134	1.49362
0.17479	0.71354	0.77484	0.92395	1.09589	1.25439	1.39057	1.50547
0.26964	0.56994	0.66492	0.88082	1.09952	1.28215	1.43054	1.55245
0.38821	0.42966	0.56927	0.85880	1.11700	1.31375	1.46710	1.59106
0.62533	0.22118	0.46558	0.84470	1.15408	1.35764	1.50966	1.63140
0.86246	0.07679	0.42647	0.82182	1.17831	1.38237	1.52847	1.64666
	Apocenter radius = 1.00000						
0.15582	0.71296	0.76238	0.88428	1.03028	1.17024	1.29360	1.39884
0.17479	0.68157	0.73709	0.87154	1.02828	1.17519	1.30277	1.41069
0.26964	0.54796	0.63577	0.83097	1.03161	1.20287	1.34358	1.45933
0.38821	0.41597	0.54771	0.81113	1.04933	1.23597	1.38302	1.50183
0.62533	0.21580	0.45138	0.80553	1.08970	1.28579	1.43362	1.55177
0.86246	0.06894	0.41541	0.79976	1.12202	1.31716	1.46114	1.57644
1.00000	0.00000	0.40623	0.78890	1.13274	1.32976	1.47100	1.58422
	Apocenter radius = 1.21816						
0.15582	0.67837	0.72103	0.82637	0.95453	1.07992	1.19216	1.28862
0.17479	0.65019	0.69823	0.81449	0.95230	1.08431	1.20080	1.30005
0.26964	0.52929	0.60672	0.77601	0.95387	1.11000	1.24049	1.34838
0.38821	0.40749	0.52735	0.75695	0.96997	1.14271	1.28109	1.39322
0.62533	0.22596	0.44007	0.75587	1.01088	1.19624	1.33806	1.45128
0.86246	0.11388	0.40697	0.76319	1.04642	1.23372	1.37363	1.48513
1.00000	0.09205	0.39930	0.76365	1.06344	1.24990	1.38793	1.49824
1.21816	0.09396	0.39476	0.75584	1.08244	1.26969	1.40417	1.51267

Table 1 (cont.)

Pericenter radius	$i = 0°$	$i = 15°$	$i = 30°$	$i = 45°$	$i = 60°$	$i = 75°$	$i = 90°$
	Apocenter radius = 1.57385						
0.15582	0.65413	0.68827	0.77390	0.88069	0.98809	1.08640	1.17213
0.17479	0.62982	0.66832	0.76285	0.87790	0.99138	1.09386	1.18242
0.26964	0.52492	0.58748	0.72565	0.87578	1.01237	1.12938	1.22733
0.38821	0.42338	0.51718	0.70533	0.88747	1.04152	1.16797	1.27142
0.62533	0.28919	0.43950	0.70263	0.92391	1.09393	1.22697	1.33363
0.86246	0.22589	0.40859	0.71513	0.95951	1.13459	1.26810	1.37451
1.00000	0.21011	0.40153	0.72236	0.97756	1.15347	1.28623	1.39206
1.21816	0.19787	0.39860	0.72984	1.00212	1.17783	1.30879	1.41350
1.57385	0.20289	0.40490	0.72861	1.03030	1.20687	1.33410	1.43718
	Apocenter radius = 2.04811						
0.15582	0.65361	0.67895	0.74600	0.83256	0.92239	1.00678	1.08182
0.17479	0.63388	0.66188	0.73570	0.82913	0.92438	1.01272	1.09055
0.26964	0.55224	0.59306	0.69922	0.82258	0.93924	1.04205	1.12967
0.38821	0.47815	0.53327	0.67630	0.82828	0.96245	1.07577	1.16995
0.62533	0.38811	0.46385	0.66704	0.85593	1.00855	1.13123	1.23064
0.86246	0.34339	0.43212	0.67678	0.88724	1.04774	1.17326	1.27397
1.00000	0.32832	0.42369	0.68479	0.90428	1.06704	1.19294	1.29375
1.21816	0.31216	0.41913	0.69714	0.92859	1.09314	1.21876	1.31929
1.57385	0.29544	0.42395	0.71141	0.96115	1.12621	1.25031	1.35013
2.04811	0.30099	0.44012	0.71590	0.99047	1.15742	1.27875	1.37788
	Apocenter radius = 2.52237						
0.15582	0.67335	0.69112	0.74173	0.81326	0.88984	0.96346	1.03010
0.17479	0.65784	0.67716	0.73212	0.80938	0.89080	0.96812	1.03749
0.26964	0.59499	0.62114	0.69655	0.79942	0.90056	0.99196	1.07121
0.38821	0.53943	0.57226	0.67126	0.80007	0.91827	1.02065	1.10711
0.62533	0.47161	0.51228	0.65495	0.81903	0.95692	1.07047	1.16366
0.86246	0.43415	0.47882	0.65936	0.84465	0.99229	1.11045	1.20618
1.00000	0.41959	0.46658	0.66551	0.85953	1.01049	1.12991	1.22631
1.21816	0.40232	0.45512	0.67685	0.88174	1.03594	1.15625	1.25312
1.57385	0.37976	0.45153	0.69429	0.91311	1.06965	1.19000	1.28702
2.04811	0.36229	0.46131	0.70963	0.94580	1.10311	1.22250	1.31953
2.52237	0.37016	0.47733	0.71474	0.96721	1.12737	1.24538	1.34273
	Apocenter radius = 2.99663						
0.15582	0.70192	0.71478	0.75227	0.80912	0.87519	0.94007	0.99976
0.17479	0.68959	0.70342	0.74374	0.80493	0.87536	0.94370	1.00604
0.26964	0.64001	0.65799	0.71098	0.79239	0.88100	0.96289	1.03508
0.38821	0.59625	0.61813	0.68476	0.78899	0.89396	0.98703	1.06682
0.62533	0.54139	0.56736	0.65940	0.80017	0.92545	1.03090	1.11858
0.86246	0.50861	0.53559	0.65576	0.82001	0.95634	1.06775	1.15901
1.00000	0.49499	0.52175	0.65901	0.83243	0.97283	1.08622	1.17863
1.21816	0.47843	0.50456	0.66749	0.85180	0.99656	1.11182	1.20537
1.57385	0.45479	0.48846	0.68352	0.88057	1.02916	1.14573	1.24022
2.04811	0.42571	0.48674	0.70188	0.91218	1.06290	1.17981	1.27502
2.52237	0.41375	0.49637	0.71351	0.93666	1.08826	1.20498	1.30091
2.99663	0.42218	0.51039	0.71869	0.95257	1.10758	1.22387	1.32075

Table 1 (cont.)

Pericenter radius	$i = 0°$	$i = 15°$	$i = 30°$	$i = 45°$	$i = 60°$	$i = 75°$	$i = 90°$
	Apocenter radius = 3.47089						
0.15582	0.73386	0.74358	0.77217	0.81630	0.87112	0.92881	0.98256
0.17479	0.72388	0.73428	0.76480	0.81203	0.87069	0.93158	0.98791
0.26964	0.68362	0.69709	0.73592	0.79730	0.87312	0.94690	1.01294
0.38821	0.64821	0.66422	0.71122	0.78913	0.88201	0.96698	1.04091
0.62533	0.60246	0.62100	0.68120	0.79262	0.90690	1.00514	1.08787
0.86246	0.57401	0.59191	0.66705	0.80698	0.93326	1.03853	1.12568
1.00000	0.56211	0.57811	0.66477	0.81691	0.94786	1.05567	1.14444
1.21816	0.54562	0.55887	0.66746	0.83320	0.96939	1.07992	1.17040
1.57385	0.52063	0.53376	0.67926	0.85868	0.99994	1.11288	1.20505
2.04811	0.48409	0.51760	0.69667	0.88815	1.03274	1.14711	1.24067
2.52237	0.46302	0.51822	0.71067	0.91205	1.05825	1.17329	1.26798
2.99663	0.45491	0.52678	0.71988	0.93090	1.07815	1.19359	1.28950
3.47089	0.46312	0.53880	0.72488	0.94289	1.09379	1.20947	1.30675
	Apocenter radius = 3.94515						
0.15582	0.76772	0.77537	0.79783	0.83243	0.87634	0.92546	0.97404
0.17479	0.75956	0.76773	0.79158	0.82839	0.87522	0.92753	0.97863
0.26964	0.72659	0.73719	0.76668	0.81323	0.87366	0.93963	1.00026
0.38821	0.69756	0.70996	0.74441	0.80184	0.87824	0.95612	1.02484
0.62533	0.65988	0.67296	0.71391	0.79451	0.89716	0.98893	1.06716
0.86246	0.63582	0.64627	0.69350	0.80195	0.91912	1.01878	1.10219
1.00000	0.62390	0.63291	0.68540	0.80941	0.93178	1.03448	1.12003
1.21816	0.60647	0.61327	0.67874	0.82254	0.95094	1.05705	1.14470
1.57385	0.57994	0.58368	0.68165	0.84443	0.97896	1.08845	1.17847
2.04811	0.54390	0.55434	0.69515	0.87116	1.01009	1.12199	1.21402
2.52237	0.50964	0.54368	0.70882	0.89377	1.03504	1.14834	1.24192
2.99663	0.49414	0.54535	0.71968	0.91233	1.05499	1.16929	1.26436
3.47089	0.48875	0.55285	0.72721	0.92714	1.07097	1.18611	1.28271
3.94515	0.49643	0.56319	0.73190	0.93630	1.08379	1.19964	1.29833
	Apocenter radius = 4.41941						
0.15582	0.80434	0.81096	0.82876	0.85585	0.89056	0.93043	0.97212
0.17479	0.79776	0.80478	0.82352	0.85215	0.88905	0.93154	0.97586
0.26964	0.77158	0.78003	0.80222	0.83747	0.88445	0.93907	0.99439
0.38821	0.74899	0.75756	0.78232	0.82459	0.88362	0.95187	1.01583
0.62533	0.71800	0.72503	0.75265	0.80926	0.89385	0.97962	1.05375
0.86246	0.69375	0.69954	0.72957	0.80547	0.91150	1.00600	1.08596
1.00000	0.68120	0.68628	0.71819	0.80850	0.92222	1.02019	1.10248
1.21816	0.66269	0.66643	0.70356	0.81782	0.93893	1.04094	1.12596
1.57385	0.63464	0.63542	0.69251	0.83588	0.96420	1.07045	1.15845
2.04811	0.59849	0.59652	0.69780	0.85948	0.99320	1.10274	1.19336
2.52237	0.55658	0.57338	0.70907	0.88037	1.01711	1.12871	1.22130
2.99663	0.53260	0.56657	0.71980	0.89811	1.03669	1.14980	1.24413
3.47089	0.52062	0.56871	0.72844	0.91283	1.05267	1.16706	1.26310
3.94515	0.51715	0.57530	0.73474	0.92466	1.06569	1.18125	1.27941
4.41941	0.52423	0.58428	0.73909	0.93172	1.07629	1.19290	1.29290